# Photocontrolled Molecular Structural Transition and Doping in Graphene
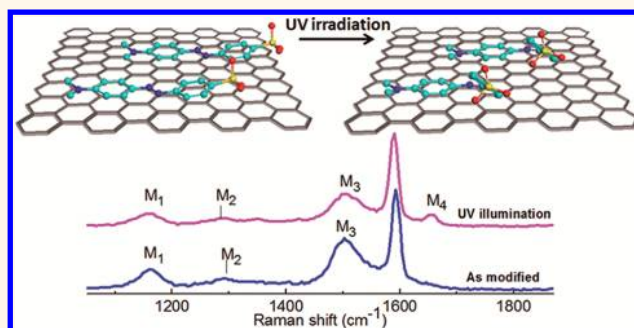
Namphung Peimyoo,[†] Jiewei Li,[†,‡] Jingzhi Shang,[†] Xiaonan Shen,[†] Caiyu Qiu,[†] Linghai Xie,[‡] Wei Huang,[‡] and Ting Yu*,[†,§]

[†]Division of Physics and Applied Physics, School of Physical and Mathematical Sciences, Nanyang Technological University, 637371, Singapore, [‡]Key Laboratory for Organic Electronics & Information Displays (KLOEID) and Institute of Advanced Materials (IAM), Nanjing University of Posts and Telecommunications, Nanjing 210046, China, and [§]Department of Physics, Faculty of Science, National University of Singapore, 117542, Singapore

Graphene, a two-dimensional sheet of carbon atoms packed into a honeycomb lattice, has remarkable mobility of charge carriers at room temperature.[1,2] Thus, one promising application of graphene is utilizing it in the electronic industry. In order to achieve high-performance graphene nanoelectronic devices, it is essential to precisely manipulate charge carriers. In view of the fact that chemical doping is an effective method to manipulate the doping level, studies on the impact of adsorbates on graphene have been attracting considerable attention. As known, chemical doping can be achieved by substitutional and surface transfer doping. Substitutional doping is a process of substituting carbon atoms in the honeycomb lattice of graphene by heterogeneous atoms such as nitrogen and boron.[3,4] Inevitably, substitutional doping may disturb the $sp^2$ hybridization of graphene. Surface transfer doping, on the other hand, would not disturb the structure of graphene and can be accomplished by adsorption of various chemical species such as metals[5,6] and organic molecules.[7−9] Surface transfer doping of organic molecules occurs through charge transfer, i.e., exchange of electrons between graphene and organic molecules. Particularly, charge transfer can occur due to the relative position of the density of state (DOS) of the highest occupied molecular orbital (HOMO) and lowest unoccupied molecular orbital (LUMO) of the adsorbed dopant and the Fermi level of graphene. If the HOMO is above the Fermi level of pristine graphene, charge will transfer from molecule to graphene, resulting in n-type doped graphene. If the LUMO is below the Fermi level, charge will transfer to the molecular adsorbate, leading to p-type doping in graphene. Experimentally, synchrotron-based high-resolution photoemission spectroscopy (PES), UV−visible spectroscopy, and Raman spectroscopy have shown evidence for charge

transfer between graphene and molecules.[8−10] Besides inducing doping in graphene, some organic molecules are able to switch their conformations under photoexcitation, which opens up a new application field, molecular graphene-based photoswitching.

Azobenzene has been extensively studied for various applications such as light-driven molecular switches,[11−14] reversible optical storage,[15] and micropatterning.[16]

## ABSTRACT



We studied chemical doping of trans- and cis-azobenzene on graphene by Raman spectroscopy. It was found that the molecule induces hole-doping in graphene through charge transfer. Moreover, the doping level in graphene can be reversibly modulated by a photocontrolled molecular conformation change. As trans-azobenzene isomerizes to the cis configuration under UV irradiation, we probe the dynamic molecular structural evolution of azobenzene on graphene by Raman spectroscopy. Raman analysis indicates the precise orientation of cis-azobenzene on the graphene surface, which brings us further comprehension of the effect of conformation change on the electronic properties of graphene. In particular, the substantial decreases of the doping level and chemical enhancement of the molecular signal are attributed to the weakening of hole transfer from molecule to graphene, owing to the lifting of the electron-withdrawing group away from the graphene. Moreover, the calculation results exhibit the favorable configuration of cis-azobenzene, which is in good agreement with Raman spectroscopic analysis. Our results highlight an approach for employing graphene as a promising platform for probing molecular conformation transition at the submolecular level by Raman spectroscopy.
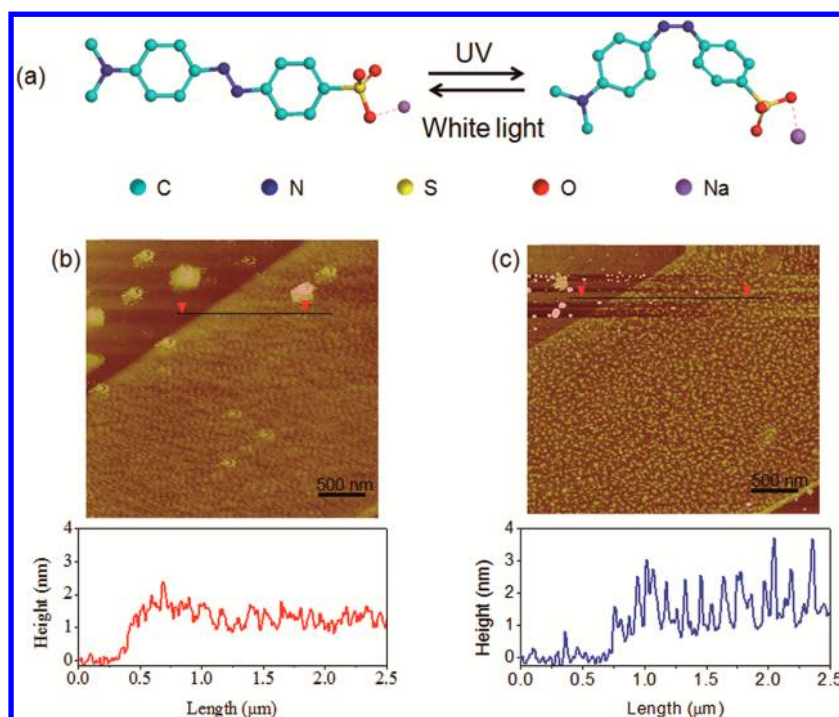
Figure 1. (a) Illustrative photoisomerization process of methyl orange (MO), where the molecular conformation changes from trans (left) to cis (right) under UV light and reverts to trans under white light. (b and c) AFM images (with height profiles) of MO-graphene before and after UV illumination, respectively.

Upon UV irradiation, the trans configuration isomerizes to cis and the cis state will reversibly transform to trans under visible light.[11] As the trans configuration is more energetically favorable than the cis configuration,[17] the cis state will thermally be transformed to trans. Theoretical studies have demonstrated the use of an azobenzene molecule contacted with Au as an electronic switch.[12,13] The calculated results showed that the conductance between the two conformations is substantially distinct. Previously, azobenzene-functionalized carbon nanotubes,[18] graphene oxide,[19] and graphene[20] have been reported, where they showed modulated conductance by UV irradiation. Previously, we presented the strong doping effect of azobenzene on graphene layers and showed that the doping is systematically thickness-dependent.[21] Raman spectroscopy is a powerful and nondestructive tool to study graphene, as it allows identifying the number of graphene layers,[22,23] monitoring the amount and type of doping,[24] and probing disorder[25,26] and strain.[27,28] In addition, recent studies on CuPc on graphene[29] and trans-azobenzene on Ag colloids[30] show that different orientations of adsorbates on graphene correspond to different Raman spectra.

In this work, we demonstrate that doping in graphene and molecular Raman scattering can be modulated by photocontrolled molecular conformation changes. Both Raman scattering and electrical transport measurements confirm that doping modulation in graphene originates from the reversibility of the molecular conformation change. Furthermore, the specific

orientation of azobenzene interacting on graphene after UV irradiation was revealed by utilizing the changes in the molecular Raman signals. On the other side, the adsorption energies of different adsorption configurations of azobenzene on graphene were calculated to examine the preferred molecular configuration. The theoretical results are consistent with the experimental data. Our studies lead to insight on two aspects: interaction between the trans-/cis-azobenzene molecule and graphene, and tunable molecular doping of graphene by a photoeffect. More importantly, these results show the unique ability of Raman spectroscopy for determining the specific configuration of azobenzene on graphene at the submolecular level, which reveals a way to sense configuration evolution of such azobenzene molecules and other switchable molecules such as stilbenes and spiropyran.

## RESULTS AND DISCUSSION

Methyl orange (MO), one type of azobenzene molecule, is used to noncovalently functionalize graphene. It is characterized by an azo group (N=N) that bridges two benzene rings. More specifically, the end of each aromatic benzene ring is substituted by a dimethyl amine group and sulfonate group, which are electron-donating and -withdrawing groups, respectively, as shown in Figure 1a. At equilibrium, azobenzene is in the trans state, with a planar structure (Figure 1a, left). UV light causes trans-azobenzene to isomerize to the cis structure, which has two benzene rings being angled with respect to each other (Figure 1a, right).
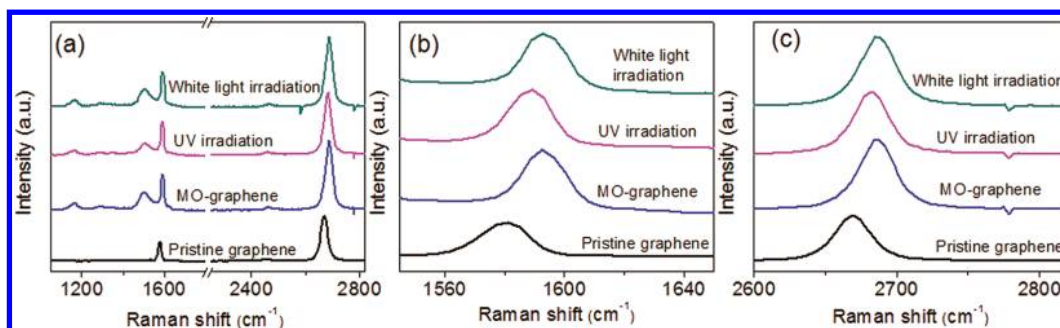
**Figure 2.** (a) Raman spectra of pristine graphene, MO-graphene, UV-irradiated MO-graphene, and UV-irradiated MO-graphene upon white light illumination. The variation of (b) the G peak and (c) the G' peak of pristine graphene, MO-graphene, UV-irradiated MO-graphene, and UV-irradiated MO-graphene upon white light illumination.

The configurations of *cis*- and *trans*-MO have been evidenced by scanning tunneling microscopy (STM) when the molecules adsorb on a Au(111) surface.[31] During the photoisomerization process, the distance between two carbon atoms that are connected by a donor and acceptor decreases from about 0.9 nm to 0.55 nm, resulting in a decrease in molecular dipole moment.[32,33] For the isomerization of azobenzene from trans geometry to cis geometry, there are two possible mechanisms: one is photoisomerization *via* inversion about one nitrogen atom in the same molecular plane; the other is isomerization *via* rotation of N=N.[34]

Figure 1b and c show the morphological change of MO film deposited on graphene before and after UV irradiation, characterized by atomic force microscopy (AFM). The thickness of pristine graphene on the $SiO_2$ substrate is ∼1 nm (Figure S1, see Supporting Information). The height profile across the marked area shows that after depositing MO on graphene the molecular film surface is smooth and the height increases to ∼1.4 nm, indicating a thickness of the molecular film of ∼0.4 nm. After UV irradiation for 2 h, the surface becomes rough and the average height increases by ∼0.5 nm, implying that the molecules transform from trans to cis configuration. In addition, by use of UV−visible absorption spectroscopy, it is found that the amounts of MO on graphene before and after UV illumination are comparable (Figure S2, see Supporting Information). Thus, no apparent desorption of MO occurs here.

Figure 2a shows a comparison among Raman spectra of pristine graphene, MO-modified graphene (MO-graphene), and MO-graphene after UV irradiation. The G peak of pristine graphene is usually observed at ∼1580 cm$^{-1}$, which arises from the high-frequency $E_{2g}$ phonon mode at the Brillouin-zone center (Γ).[22] The G' (or 2D) peak, usually observed at ∼2670 cm$^{-1}$ (under 2.33 eV excitation), is a second-order vibration caused by the scattering of two phonons at the zone boundary.[35] Raman spectra can effectively indicate the type and the amount of doping through the change of position and line width of the G peak as well as the shift of the G' peaks, referring to those of the pristine sample.[24] After the modification by MO, several MO bands appear in the range between 1050 and 1630 cm$^{-1}$, as shown in Figure 2a. It is noted that there is no obvious peak around 1350 cm$^{-1}$ after deposition of MO on graphene, which indicates the absorption process of MO on graphene does not destroy the structure of graphene. In our previous study, we have shown MO induced hole-doping in graphene through charge transfer, and the doping is highest in monolayer graphene and decreased with increasing number of layers.[21] Although MO contains both an electron donor and electron acceptor, overall the MO molecule is an electron acceptor because the sulfonate group is a strong electron-withdrawing group, whereas the dimethyl amino group is a relatively weak electron-donating group.

The changes of the G peak after MO deposition and UV illumination are shown in Figure 2b. The G peak after MO deposition shifts to ∼1592 cm$^{-1}$ from ∼1580 cm$^{-1}$. After UV illumination the G peak moves back ∼3 cm$^{-1}$ toward the lower energy region. The G' peak also shifts toward higher energy by ∼10 cm$^{-1}$ after MO deposition and shifts back ∼2.5 cm$^{-1}$ after UV exposure (Figure 2c). The reverse shifts of the G and G' peak after UV irradiation clearly indicate the decreased doping in graphene. It was reported that UV illumination effectively modulates the doping level in graphene through the conformation change of DR1-functionalized pyrene.[20] Here, the downshift of both the G and G' peak for the UV-irradiated sample is also due to the molecular conformation change under UV light from trans to cis, which causes the weakening of the interaction between graphene and the molecule. After white light illumination, the G and G' peaks shift back to positions similar to those of MO-graphene, which indicates the recovery of doping in graphene. This doping modulation by UV and white light has been further confirmed by the electrical transport measurements of a back gate MO-graphene transistor (Figure S3, see Supporting Information). Similar transport behavior was also found in graphene functionalized with disperse red 1; however, the additional pyrene group was used as the linker there.[20]
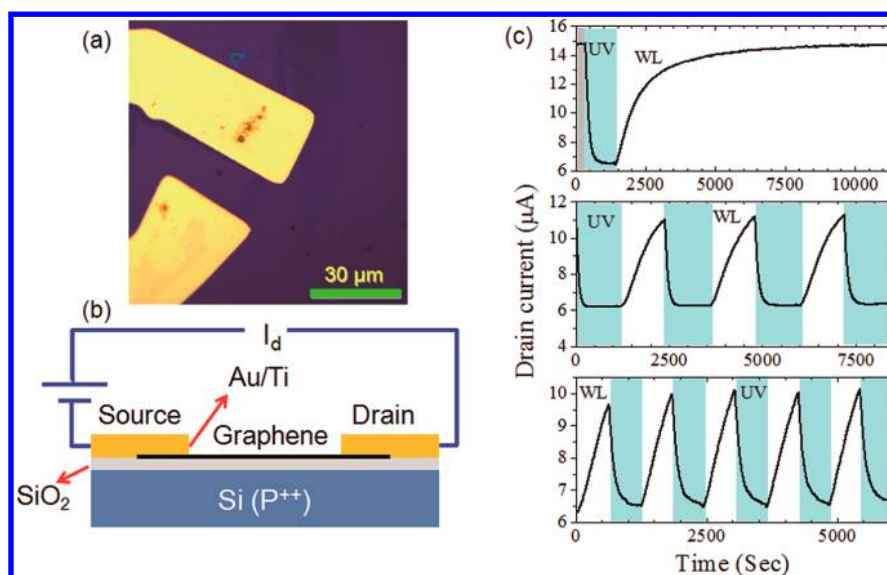
**Figure 3.** (a) Optical image of MO-graphene device. (b) Schematic of the photoswitching setup. (c) Drain current *versus* irradiation time curves.

Moreover, the photoswitching measurement was carried out to further examine the effect of light on doping in MO-graphene samples (Figure 3). Figure 3a and b show an optical image of the MO/graphene device and the schematic of the experimental setup. The top panel in Figure 3c presents the drain current evolution with time. In the left gray region (0−350 s), the current of the as-prepared MO-graphene sample was measured in a dark room and stayed around 14.8 $\mu$A. Then, UV light was turned on for ∼1000 s (denoted by the blue shadow), and the current was found to be stable at 6.5 $\mu$A. This process corresponds to isomerization from trans to cis state. The conversion time constant is ∼110 s, obtained by a monoexponential fit, as shown in Figure S3c. After that, UV light was removed and white light was introduced. With the transformation from the cis to trans state, the current increased and remained around the value before UV irradiation. Thus, the light-driven doping in MO-graphene is reversible. Furthermore, multiple photoswitching measurements have been performed at two periods, 1200 s (UV 600 s/WL 600 s) and 2400 s (UV 1200 s/WL 1200 s), as shown in the middle and bottom panels, respectively. The repeatable and reversible rise and decrease of drain current demonstrates the stability of conductance modulation of the present MO-graphene system.

To exploit the structural evolution of MO on graphene during UV illumination, the detailed Raman features of as-modified and the UV-illuminated samples are analyzed. Figure 4a shows Raman peaks of molecular signals observed in the MO-graphene and irradiated MO-graphene samples. Note that the molecular signals were not detectable on the SiO$_2$/Si substrate (Figure S4, see Supporting Information), indicating that these MO signals were chemically enhanced on the graphene substrate, which has been previously reported in various organic molecule-graphene systems.[36,37] Upon UV illumination, the peak positions of MO remain the same, while the intensities alter (Figure 4a). The inset is the molecular structure of MO. The peak at 1158 cm$^{-1}$ (labeled M$_1$) is assigned to the stretching mode of C−S, C−C, and S=O.[30,38] The weak peak at 1290 cm$^{-1}$, denoted as M$_2$, is ascribed to the stretching mode of C−N, and the most intense peak at ∼1500 cm$^{-1}$ (M$_3$) originates from the stretching mode of an N-aromatic ring.[30] After UV irradiation, the new peak, labeled as M$_4$, appears at 1650 cm$^{-1}$, which was also observed in the Raman spectra of MO adsorbed on Ag particles.[30] The appearance of the M$_4$ peak in the UV-illuminated sample could be due to the fact that the vibrational mode becomes polarization allowed after the structural change. A detailed study on this mode is needed. The relative intensity ratios between molecular Raman peaks and the G peak were thoroughly analyzed and utilized to trace the transition of the molecular configuration after illumination with UV light.

Figure 4b−e show the comparison of the normalized intensity ratio of the molecular peaks and the G peak, $I(M_1)/I(G)$, $I(M_2)/I(G)$, $I(M_3)/I(G)$, and $I(M_4)/I(G)$, respectively, before and after UV irradiation. Note that $I(M_1)/I(G)$, $I(M_2)/I(G)$, and $I(M_3)/I(G)$ are normalized by their values after modification, whereas $I(M_4)/I(G)$ is normalized to its value after the UV irradiation. $I(M_1)/I(G)$, $I(M_2)/I(G)$, and $I(M_3)/I(G)$ decrease by 34%, 19%, and 28%, respectively, after successive UV irradiation, indicating the occurrence of molecular conformation transition. As MO contains aromatic rings, it interacts with graphene *via* $\pi-\pi$ interactions; thus the MO molecule in trans configuration is favorable to align parallel to the graphene surface, as schematically shown in Figure 5 (left). The reductions of $I(M_1)/I(G)$
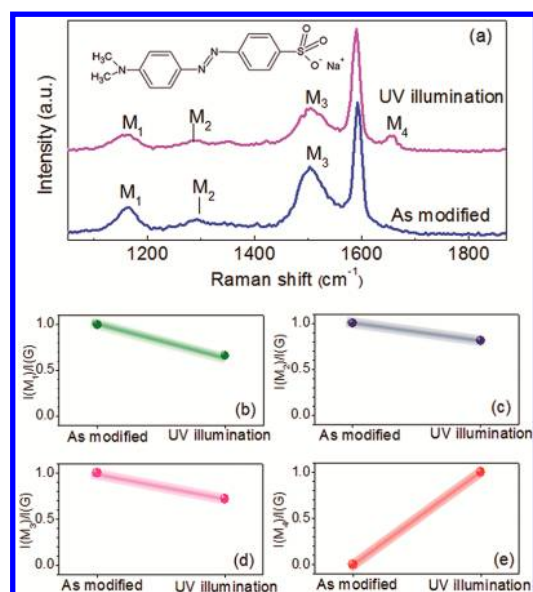
Figure 4. (a) Raman spectra of MO-graphene and UV-irradiated MO-graphene presenting the molecular Raman peaks, denoted as $M_1$, $M_2$, $M_3$, and $M_4$. The inset is the molecular structure of MO. (b–e) Normalized intensity ratio of molecular peaks to the G peak after modification and UV irradiation: (b) $I(M_1)/I(G)$, (c) $I(M_2)/I(G)$, (d) $I(M_3)/I(G)$, and (e) $I(M_4)/I(G)$.
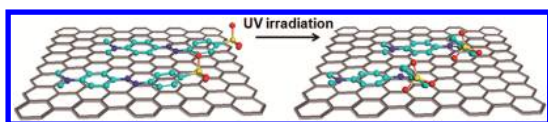


Figure 5. Schematic diagram showing the adsorption of MO on graphene. Before UV illumination the molecule interacts with graphene via a $\pi-\pi$ interaction (left). UV light alters the MO conformation into the cis configuration, in which the sulfonate group and its corresponding aromatic ring are lifted from the graphene surface (right).

and $I(M_3)/I(G)$, which are related to vibrational modes of C—S/S=O and an N-aromatic ring, respectively, suggest that after UV irradiation a sulfonic functional group with its corresponding benzene ring moves upward from the graphene surface to form a cis configuration (Figure 5 right). The different degrees of the reduction of the ratios are attributed to distinct interactions of molecular vibrational modes on graphene. The reduction proportions of $I(M_1)/I(G)$ and $I(M_3)/I(G)$ are larger than that of $I(M_2)/I(G)$, implying that $M_1$ and $M_3$ vibrational modes are further away from the graphene surface than the $M_2$ mode after UV illumination.

The preferable cis configuration as mentioned above can be explained by the distinct interaction of functional groups substituted at each side of the benzene ring on graphene. As a result of the dimethyl amine group being as hydrophobic as graphene, it adheres to graphene via a hydrophobic interaction. On the other hand, the sulfonate group is hydrophilic; thus a repulsive interaction between it and graphene exists. Therefore, after UV irradiation, *trans*-MO changes to a
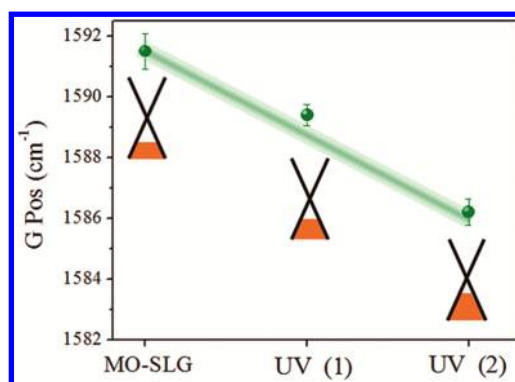


Figure 6. G peak positions of modified graphene and UV-irradiated modified graphene in methods 1 and 2.

cis configuration, resulting in the lifting of the sulfonate group and the corresponding aromatic ring owing to the repulsive force, whereas another aromatic ring with a dimethyl amine group prefers to remain adsorbing parallel to the graphene surface. The observed downshifts of the G and G′ peaks are consequences of conformation transition. Since the sulfonic group is a strong electron-withdrawing group, resulting in p-doping in graphene, once the electron donor lifts upward, the hole transfer efficiency from the molecule to graphene is significantly decreased. As charge transfer is one of the most essential requirements for the occurrence of chemical enhancement, the decrease of hole transfer will weaken the chemical enhancement. Thus the reduction of Raman intensity of $M_1$, $M_2$, and $M_3$ after UV illumination was observed as mentioned previously.

In ref 20, the azobenzene is not directly adsorbed on the graphene surface but connected to pyrene, which interacts on the graphene surface; thus the azobenzene molecule can freely change conformations under UV illumination. However in our work, the MO molecule directly anchors onto the graphene surface via a $\pi-\pi$ interaction. To isomerize from trans to cis form, the MO molecule needs to overcome the $\pi-\pi$ interaction. Thus, it is plausible that the MO may not be capable of transforming its configuration completely. In order to clarify the influence of the $\pi-\pi$ interaction on the molecular conformation change, we compared the doping between the two methods. In method 1, MO was deposited on the graphene surface and then dried at room temperature, followed by rinsing to remove unabsorbed molecules. The UV illumination was conducted afterward for 2 h. For method 2, the MO solution was drop cast on graphene and UV illumination was simultaneously carried out as long as in method 1.

Figure 6 compares the G peak positions of MO-graphene and UV-irradiated MO-graphene for methods 1 and 2. Note that in order to ensure doping homogeneity, the G peak positions were extracted from Raman spectra from 10 different points, as Raman spectra on different points from the same sample can
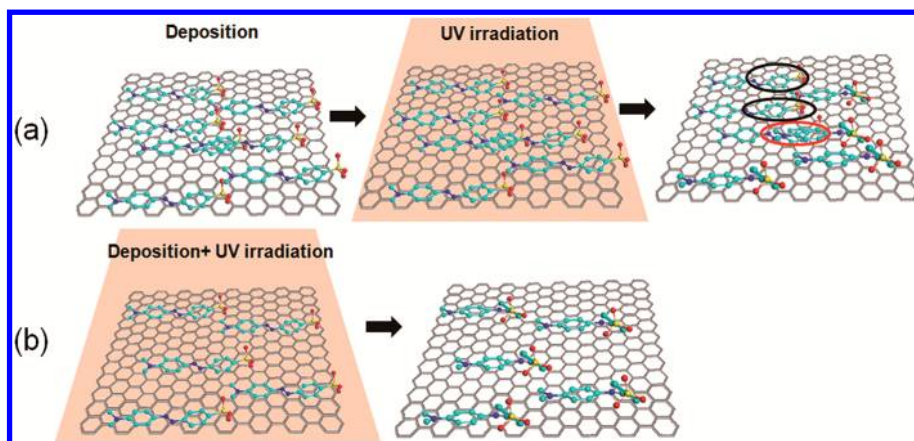
**Figure 7.** Schematic diagrams showing deposition and photoisomerization processes for two methods. (a) Method 1: the MO molecules were spin coated onto graphene and then dried at room temperature. The UV irradiation was carried out afterward. (b) Method 2, the MO solution was drop cast onto graphene and UV illumination was simultaneously performed. In the case of method 1, as the molecules were deposited onto the graphene surface due to $\pi-\pi$ interactions, first, it is plausible that after UV exposure, some molecules may not be able to transform to the cis state (black circle). The red circle shows the overlapping of molecules that encounter the transition of MO.

vary even in pristine graphene.[39] Referring to that of the as-modified sample, the G peak positions after UV irradiation downshift by $\sim$3 and $\sim$6 cm$^{-1}$ for a sample under conditions 1 and 2, respectively. The estimated hole concentration can be quantified with respect to the shift of the G peak caused by electrostatic doping.[24] The carrier concentration is $\sim$5 $\times$ 10$^{13}$ cm$^{-2}$ after functionalization. UV light significantly decreases the carrier concentration to $\sim$4 $\times$ 10$^{13}$ and $\sim$2.8 $\times$ 10$^{12}$ cm$^{-2}$ for methods 1 and 2, respectively. The insets are schematic drawings of electronic structures corresponding to the observed G peak positions. In the modified sample, the Fermi energy ($E_F$) greatly shifts away from the Dirac point. After the UV irradiation, the shift of $E_F$ becomes smaller and associates with the G peak position.

Figure 7a and b represent the schematic diagram describing the photoisomerization processes for methods 1 and 2, respectively. The larger downshift of the G peak position in method 2 compared to that of method 1 could be elucidated by the following reasons. For method 1, as molecules first adsorb on graphene in the trans configuration before carrying out UV exposure, it is reasonable that a $\pi-\pi$ interaction between them counteracts the conformation transition. Thus, some portions of molecules may not be able to convert their structure into the cis configuration (black circles). Besides the $\pi-\pi$ interaction, the possible overlapping of some molecules during deposition could prevent them from altering their structure from trans to cis (red circle). In contrast, for method 2 the UV irradiation was performed instantly after deposition. Presumably, before the MO adheres to the graphene surface, the molecules are able to alter their structure freely from trans to cis configuration. As a result, the proportion of cis-azobenzene in method 2 is more substantial than that of method 1. Owing to less disturbance of the $\pi-\pi$

interaction, it is sensible to assume that the distance between the lifted part of the molecule and graphene in method 2 is relatively larger than that of the former method. According to the considerations above, the degree of charge transfer from graphene to MO in method 2 is smaller than that of method 1. This result indicates that the interaction between graphene and the molecule can affect the molecular conformation transition.

In the following, in order to verify the Raman analysis on the geometry of cis-MO interacting on a graphene surface, we calculated the adsorption energies of the molecule with different geometries (see Supporting Information for the calculation details). Figure 8 shows the three optimized adsorption configurations of MO on graphene. In configuration 1, the MO molecule is in trans configuration, lying on the graphene surface (Figure 8a). In the case of the cis state, we consider two possible configurations. For configuration 2 (cis form), one aromatic benzene ring attached to a sulfonate group is lying on the graphene surface, while the other benzene ring, with a dimethyl amine group, is lifted upward (Figure 8b). Configuration 3, another cis form, contradicts configuration 2, in that one aromatic benzene ring connected with a dimethyl amine group is parallel to the graphene surface, while the other part is lifted (Figure 8c). The adsorption energy is defined by the following equation:

$$\Delta E_{absorption} = E_{total} - E_{graphene} - E_{molecule}$$

where $E_{total}$ is the total energy of the optimized molecule-doped graphene system, $E_{graphene}$ is the total energy of pristine graphene, and $E_{molecule}$ is the energy of the isolated molecular adsorbate.

The summarized results including adsorption energies and MO-graphene distances corresponding to the three configurations are shown in Table 1. It is worth
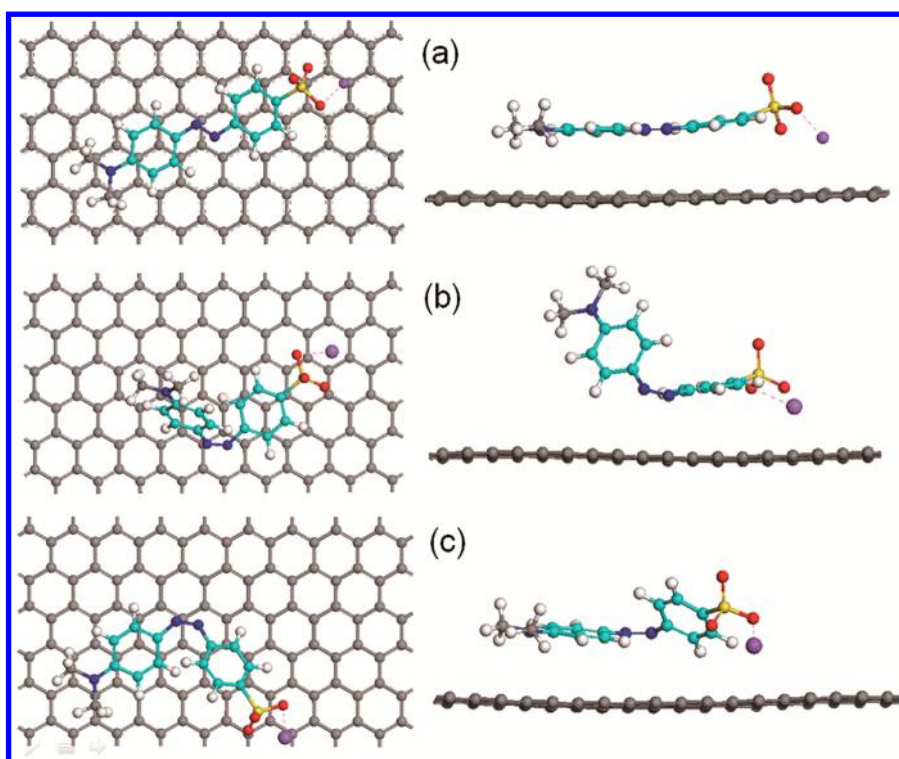
**Figure 8.** Top view (left) and side view (right) of optimized adsorption configurations of MO on graphene. (a) Configuration 1: *trans*-MO adheres to the graphene surface where two aromatic benzene rings and graphene are in-plane. (b) Configuration 2: *cis*-MO adsorbs on graphene where one aromatic ring with a sulfonic group aligns parallel with respect to the graphene surface while another aromatic ring moves upward. (c) Configuration 3: *cis*-MO adsorbs on graphene where one aromatic ring with a dimethyl amine group interacts with graphene while another aromatic ring lifts upward.

**TABLE 1. Calculated Adsorption Energies of Three Configurations of MO Adsorbed on Graphene**

| configuration | adsorption energy (eV) | distance (Å) |
|---|---|---|
| 1 | −3.95 | 3.09 |
| 2 | −1.90 | 3.05 |
| 3 | −2.90 | 3.46 |

noting that the distance between the molecule and graphene is measured perpendicularly from one carbon atom in graphene to the closest N atom in the azo group. According to the theoretical calculation, the adsorption energy of configuration 1 (trans configuration) is the highest, indicating that it is the most stable configuration owing to more functional groups interacting with graphene. For cis geometries, the adsorption energy in configuration 2 is lower than that of configuration 3 by 1 eV. Consequently, the molecule is more energetically favorable to alter its conformation to configuration 3 than configuration 2 after UV irradiation. The theoretical results correspond with the Raman investigation that the sulfonic group, with its corresponding aromatic ring, prefers to lift upward into the air to obtain a cis configuration. According to the calculations, the dihedral angle between the two benzene rings of isolated *cis*-azobenzene is ∼90° (angle at the conical intersection);[40,41] in contrast, the dihedral angle obtained from our calculation for configuration 3 is ∼45°. The decrease

of the dihedral angle is attributed to the passivated isomerization process by the interaction between graphene and the molecule. In order to compare the electron-accepting capability of *trans*- and *cis*-MO, the electron affinities were calculated. The electron affinity (vertical excitations)[42] of *trans*-MO is about 1.06 eV, and that for *cis*-MO is 0.96 eV. This indicates that the trans configuration can attach electrons easier than the cis configuration. Thus, the degree of charge transfer from graphene to *trans*-MO is higher than that to *cis*-MO, which is also in good agreement with Raman scattering studies.

## CONCLUSIONS

In summary, the modulation of doping in graphene and the Raman intensity of molecules has been demonstrated by the molecular conformation transition *via* the photoeffect. The *trans*-MO-modified graphene imposes stronger doping than that of *cis*-MO, and this doping modulation is reversible, as evidenced by the shift of the G peak and electrical transport characteristics. Under illumination with UV and white light, the MO-graphene transistor shows the switching behavior of the conductance, thus affirming that the reversibly modulated doping in graphene originates from reversible photoisomerization of azobenzene. More importantly, we introduce a way to identify the precise *cis*-MO geometry, which is done by analyzing the change

of intensities of molecular Raman peaks before and after UV irradiation. The reductions of doping in graphene and molecular Raman signals when MO transforms to the cis configuration arise from partial lifting of the molecules, *i.e.*, the weakening of charge transfer. The calculation results agree well with experimental data, affirming that Raman spectroscopy is an effective route to particularly identify the configuration of MO. We believe that this work opens up research on optical modulated doping in graphene and more importantly extends potentials of graphene as a unique platform for studying molecular structural evolution at a submolecular level.

## EXPERIMENTAL DETAILS

Graphene monolayer was prepared by mechanical cleavage from highly ordered pyrolytic graphite[43] and then transferred onto a $SiO_2$/Si wafer. Single-layer graphene is identified by Raman[22,23,26] and optical contrast spectroscopy.[44] 4-Dimethylaminoazobenzene-4-sulfonic acid, or methyl orange, was used to functionalize graphene. The MO solution with a concentration of $2 \times 10^{-5}$ M was selected for graphene modification to generate a monolayer thick molecular film on graphene.[21] The MO solution was prepared in dimethylformamide (DMF) solution and was then deposited onto a graphene sheet by spin coating at 2000 rpm for 2 min. After functionalization, the sample was rinsed with DMF to remove unadsorbed molecules.

Raman measurements were performed using a WITEC CRM200 Raman system with a 532 nm laser source. The incident laser power was 0.3 mW to prevent decomposition of the molecules and thermal effects. The laser spot size was about 0.5 $\mu$m in diameter using a 100$\times$ objective lens. Photoisomerization was performed at ambient pressure by illumination of the MO-graphene sample using a ~1.25 mW/cm$^2$ UV lamp with a 356 nm line for 2 h to alter the conformation of MO from trans to cis. To isomerize from cis to trans, the sample was illuminated under white light from a tungsten lamp with an intensity of 0.65 W/cm$^2$ for 3 h. The distance between the samples and light sources was maintained at 10 cm. The doping modulation in graphene was thoroughly monitored by Raman spectroscopy.

The steady-state absorption spectrum was determined by an UV−vis spectrophotometer (Cary 100Bio, Varian). For preparing the field effect transistor, monolayer graphene was first exfoliated on p-Si substrates with a 300 nm $SiO_2$ layer. After that, a double-layer photoresist (MMA and PMMA) was spin-coated onto the sample for the patterning process. The source and drain electrodes were designed by means of standard electron-beam lithography. To create two-probe devices, two contacts consisting of Ti/Au (5 nm/60 nm) were deposited by electron beam evaporator. The heavily p-doped (boron) Si served as a global back gate in the FET configuration. The drain current ($I_d$) *versus* the gate voltage ($V_g$) was recorded by sweeping back-gate bias at a constant drain−source bias ($V_d = 0.1$ V). Photoswitching measurements were performed under $V_g = 0$ V and $V_d = 0.1$ V.

*Conflict of Interest:* The authors declare no competing financial interest.

*Supporting Information Available:* Figures S1−S4 and computational details. This material is available free of charge *via* the Internet at http://pubs.acs.org.

## REFERENCES AND NOTES

1. Du, X.; Skachko, I.; Barker, A.; Andrei, E. Y. Approaching Ballistic Transport in Suspended Graphene. *Nat. Nanotechnol.* **2008**, *3*, 491–495.
2. Bolotin, K. I.; Sikes, K. J.; Jiang, Z.; Klima, M.; Fudenberg, G.; Hone, J.; Kim, P.; Stormer, H. L. Ultrahigh Electron Mobility in Suspended Graphene. *Solid State Commun.* **2008**, *146*, 351–355.
3. Guo, B.; Liu, Q.; Chen, E.; Zhu, H.; Fang, L.; Gong, J. R. Controllable N-Doping of Graphene. *Nano Lett.* **2010**, *10*, 4975–4980.
4. Wei, D.; Liu, Y.; Wang, Y.; Zhang, H.; Huang, L.; Yu, G. Synthesis of N-Doped Graphene by Chemical Vapor Deposition and Its Electrical Properties. *Nano Lett.* **2009**, *9*, 1752–1758.
5. Lee, J.; Novoselov, K. S.; Shin, H. S. Interaction between Metal and Graphene: Dependence on the Layer Number of Graphene. *ACS Nano* **2011**, *5*, 608–612.
6. Gierz, I.; Riedl, C.; Starke, U.; Ast, C. R.; Kern, K . Atomic Hole Doping of Graphene. *Nano Lett.* **2008**, *8*, 4603–4607.
7. Dong, X.; Fu, D.; Fang, W.; Shi, Y.; Chen, P.; Li, L. J. Doping Single-Layer Graphene with Aromatic Molecules. *Small* **2009**, *5*, 1422–1426.
8. Chen, W.; Chen, S.; Qi, D. C.; Gao, X. Y.; Wee, A. T. S. Surface Transfer P-Type Doping of Epitaxial Graphene. *J. Am. Chem. Soc.* **2007**, *129*, 10418–10422.
9. Voggu, R.; Das, B.; Rout, C. S.; Rao, C. N. R. Effects of Charge Transfer Interaction of Graphene with Electron Donor and Acceptor Molecules Examined Using Raman Spectroscopy and Cognate Techniques. *J. Phys.: Condens. Matter* **2008**, *20*, 472204.
10. Das, B.; Voggu, R.; Rout, C. S.; Rao, C. N. R. Changes in the Electronic Structure and Properties of Graphene Induced by Molecular Charge-Transfer. *Chem. Commun.* **2008**, *41*, 5155–5157.
11. Hugel, T.; Holland, N. B.; Cattani, A.; Moroder, L.; Seitz, M.; Gaub, H. E. Single-Molecule Optomechanical Cycle. *Science* **2002**, *296*, 1103–1106.
12. Zhang, C.; Du, M. H.; Cheng, H. P.; Zhang, X. G.; Roitberg, A. E.; Krause, J. L. Coherent Electron Transport through an Azobenzene Molecule: A Light Driven Molecular Switch. *Phys. Rev. Lett.* **2004**, *92*, 158301.
13. Zhang, C.; He, Y.; Cheng, H. P.; Xue, Y.; Ratner, M. A.; Zhang, X. G.; Krstic, P. Current-Voltage Characteristics through a Single Light-Sensitive Molecule. *Phys. Rev. B* **2006**, *73*, 125445.
14. del Valle, M.; Gutiérrez, R.; Tejedor, C.; Cuniberti, G. Tuning the Conductance of a Molecular Switch. *Nat. Nanotechnol.* **2007**, *2*, 176–179.
15. Hagen, R.; Bieringer, T. Photoaddressable Polymers for Optical Data Storage. *Adv. Mater.* **2001**, *13*, 1805–1810.
16. Ubukata, T.; Hara, M.; Ichimura, K.; Seki, T. Phototactic Mass Transport in Polymer Films for Micropatterning and Alignment of Functional Materials. *Adv. Mater.* **2004**, *16*, 220–223.
17. Schulze, F. W.; Petrick, H. J.; Cammenga, H. K.; Klinge, H. Thermodynamic Properties of Structural Analogues Benzo[c]cinnoline, Trans-azobenzene, and Cis-azobenzene. *Phys. Chem. Neue Fol.* **1977**, *107*, 1–19.
18. Simmons, J. M.; In, I.; Campbell, V. E.; Mark, T. J.; Léonard, F.; Gopalan, P.; Eriksson, M. A. Optically Modulated Conduction in Chromophore-Functionalized Single-Wall Carbon Nanotubes. *Phys. Rev. Lett.* **2007**, *98*, 086802.
19. Zhang, X.; Feng, Y.; Huang, D.; Li, Y.; Feng, W. Investigation of Optical Modulated Conductance Effects Based on a Graphene Oxide-Azobenzene Hybrid. *Carbon* **2010**, *48*, 3236–3241.
20. Kim, M.; Safron, N. S.; Huang, C.; Arnold, M. S.; Gopalan, P. Light-Driven Reversible Modulation of Doping in Graphene. *Nano Lett.* **2012**, *12*, 182–187.
21. Peimyoo, N.; Yu, T.; Shang, J. Z.; Cong, C. X.; Yang, H. P. Thickness-Dependent Azobenzene Doping in Mono- and Few-Layer Graphene. *Carbon* **2012**, *50*, 201–208.
22. Ferrari, A. C.; Meyer, J. C.; Scardaci, V.; Casiraghi, C.; Lazzeri, M.; Mauri, F.; Piscanec, S.; Jiang, D.; Novoselov, K. S.; Roth, S.;

*et al.* Raman Spectrum of Graphene and Graphene Layers. *Phys. Rev. Lett.* **2006**, *97*, 187401.

23. Gupta, A.; Chen, G.; Joshi, P.; Tadigadapa, S.; Eklund., P. C. Raman Scattering from High-Frequency Phonons in Supported N-Graphene Layer Films. *Nano Lett.* **2006**, *6*, 2667–2673.

24. Das, A.; Pisana, S.; Chakraborty, B.; Piscanec, S.; Saha, S. K.; Waghmare, U. V.; Novoselov, K. S.; Krishnamurthy, H. R.; Geim, A. K.; Ferrari, A. C.; *et al.* Monitoring Dopants by Raman Scattering in an Electrochemically Top-Gated Graphene Transistor. *Nat. Nanotechnol.* **2008**, *3*, 210–215.

25. Ni, Z. H.; Wang, Y. Y.; Yu, T.; Shen, Z. X. Raman Spectroscopy and Imaging of Graphene. *Nano Res.* **2008**, *1*, 273–291.

26. Ferrari, A. C. Raman Spectroscopy of Graphene and Graphite: Disorder, Electron-Phonon Coupling, Doping and Nonadiabatic Effects. *Solid State Commun.* **2007**, *143*, 47–57.

27. Yu, T.; Ni, Z. H.; Du, C.; You, Y. M.; Wang, Y. Y.; Shen, Z. X. Raman Mapping Investigation of Graphene on Transparent Flexible Substrate: The Strain Effect. *J. Phys. Chem. C* **2008**, *112*, 12602–12605.

28. Ni, Z.; Yu, T.; Lu, Y. H.; Wang, Y.; Feng, Y.; Shen, Z. Uniaxial Strain on Graphene: Raman Spectroscopy Study and Band-Gap Opening. *ACS Nano* **2008**, *2*, 2301–2305.

29. Ling, X.; Wu, J.; Xu, W.; Zhang, J. Probing the Effect of Molecular Orientation on the Intensity of Chemical Enhancement Using Graphene-Enhanced Raman Spectroscopy. *Small* **2012**, *8*, 1365–1372.

30. Zhang, A.; Fang, Y. Influence of Adsorption Orientation of Methyl Orange on Silver Colloids by Raman and Fluorescence Spectroscopy: pH Effect. *Chem. Phys.* **2006**, *331*, 55–60.

31. Henzl, J.; Bredow, T.; Morgenstern, K. Irreversible Isomerization of the Azobenzene Derivate Methyl Orange on Au(111). *Chem. Phys. Lett.* **2007**, *435*, 278–282.

32. Brozozowski, L.; Sargent, E. H. Azobenezene for Photonic Network Applications: Third-Order Nonlinear Optical Properties. *J. Mater. Sci.* **2001**, *12*, 483–489.

33. Nero, D.; de Araujo, R. E.; Gomes, A. S. L.; de Melo, C. P. Theoretical and Experimental Investigation of the Second Hyperpolarizabilities of Methyl Orange. *J. Chem. Phys.* **2005**, *122*, 104506.

34. Chang, C. W.; Lu, Y. C.; Wang, T. T.; Diau, E. W. G. Photoisomerization Dynamics of Azobenzene in Solution with $S_1$ Excitation: A Femtosecond Fluorescence Anisotropy Study. *J. Am. Chem. Soc.* **2004**, *126*, 10109–10118.

35. Malard, L. M.; Pimenta, M. A.; Dresselhaus, G.; Dresselhaus, M. S. Raman Spectroscopy in Graphene. *Phys. Rep* **2009**, *473*, 51–87.

36. Ling, X.; Xie, L. M.; Fang, Y.; Xu, H.; Zhang, H. L.; Kong, J.; Dresselhaus, M. S.; Zhang, J.; Liu, Z. Can Graphene be Used as a Substrate for Raman Enhancement? *Nano Lett.* **2010**, *10*, 553–561.

37. Xie, L; Ling, X.; Fang, Y.; Zhang, J.; Liu, Z. Graphene as a Substrate To Suppress Fluorescence in Resonance Raman Spectroscopy. *J. Am. Chem. Soc.* **2009**, *131*, 9890–9891.

38. Zhao, B.; Hua, H.; Haddan, R. C. Synthesis and Properties of a Water-Soluble Single-Walled Carbon Nanotube-Poly(m-aminobenzene sulfonic acid) Graft Copolymer. *Adv. Funct. Mater.* **2004**, *14*, 71–76.

39. Casiraghi, C.; Pisana, S.; Novoselov, K. S.; Geim, A. K.; Ferrari, A. C. Raman Fingerprint of Charged Impurities in Graphene. *Appl. Phys. Lett.* **2007**, *98*, 233108.

40. Cembran, A.; Bernardi, F.; Garavelli, M.; Gagliardi, L.; Orlandi, G. On the Mechanism of the Cis-Trans Isomerization in the Lowest Electronic States of Azobenzene: S0, S1, and T1. *J. Am. Chem. Soc.* **2004**, *126*, 3234–3243.

41. Wei, E.; Diau, G. A New Trans-to-Cis Photoisomerization Mechanism of Azobenzene on the S1(n,$\pi$*) Surface. *J. Phys. Chem. A* **2004**, *108*, 950–956.

42. Ran, X. Q.; Feng, J. K.; Ren, A. M.; Li, W. C.; Zou, L. Y.; Sun, C. C. Theoretical Study on Photophysical Properties of Ambipolar Spirobifluorene Derivatives as Efficient Blue-Light-Emitting Materials. *J. Phys. Chem. A* **2009**, *113*, 7933–7939.

43. Novoselov, K. S.; Geim, A. K.; Morozov, S. V.; Jiang, D.; Zhang, Y.; Dubonos, S. V.; Grigorieva, I. V.; Firsov, A. A. Electric Field Effect in Atomically Thin Carbon Films. *Science* **2004**, *306*, 666–669.

44. Ni, Z. H.; Wang, H. M.; Kasim, J.; Fan, H. M.; Yu, T.; Wu, Y. H.; Feng, Y. P.; Shen, Z. X. Graphene Thickness Determination Using Reflection and Contrast Spectroscopy. *Nano Lett.* **2007**, *7*, 2758–2763.